Environmental Technology & Innovation 31 (2023) 103198

Contents lists available at ScienceDirect

Environmental Technology & Innovation

journal homepage: www.elsevier.com/locate/eti

Purification of emulsified oily polluted waters with modified melamine foams

Sarah Hailan [a], Patrik Sobolciak [a], Peter Kasak [a], Anton Popelka [a], Yongfeng Tong [b], Samer Adham [c], Igor Krupa [a,d,*]

[a] Center for Advanced Materials, Qatar University, P.O. Box 2713, Doha, Qatar
[b] Qatar Environment and Energy Research Institute, Hamad Bin Khalifa University, Qatar
[c] ConocoPhillips Global Water Sustainability Center, Qatar Science and Technology Park, P.O. Box 24750, Doha, Qatar
[d] Materials Science and Technology Graduate Program, College of Arts and Sciences, Qatar University, 2713, Doha, Qatar

ARTICLE INFO

Article history:
Received 8 February 2023
Received in revised form 29 April 2023
Accepted 7 May 2023
Available online 12 May 2023

Keywords:
Demulsification
Produced water
Melamine foams
Ferric chloride
Superhydrophobicity
Diffusion
Adsorption

ABSTRACT

Oil and gas industry operations produce tremendous amounts of wastewater (produced water; PW). Tertiary treatment of the PW in the final treatment stage is challenging due to the presence of colloids with sizes < 500 nm and a low concentration target for the effluent of <10 mg/L. This study was focused on the purification of colloidal PW with modified melamine foams (MFs) and ferric chloride. The modified MFs exhibited superhydrophobic and superoleophilic character due to increasing roughness and complexation of Fe^{3+} ions within the MF structure. The modified MF showed separation efficiencies up to 86 ± 3% for emulsions containing 120 ppm carbon. The Fe^{3+} cations changed the hydrophilicities of the foams and made them highly hydrophobic, and they also contributed significantly to the adsorption of negatively charged species, such as crude oil droplets modified with an anionic surfactant (sodium dodecyl sulfate). The demulsification mechanism involved multiple diffusion processes run over different time scales, including diffusion of an emulsion into the foam and diffusion of the oil droplets within the foam, combined with parallel adsorption of the oil droplets onto the solid skeleton of the foam. The adsorption capacity of the MFs increased linearly with increasing initial concentration of crude oil content in the PW. The MFs were reusable for six consecutive cycles.
© 2023 The Authors. Published by Elsevier B.V. This is an open access article under the CC BY license (http://creativecommons.org/licenses/by/4.0/).

0. Introduction

Water is used and produced in the oil and gas industry as a part of the upstream and downstream operations related to hydrocarbon extraction and processing (Igunnu and Chen, 2014; Adham et al., 2018a). The water associated with oil extraction is called produced water (PW), whereas water generated as a byproduct of hydrocarbon processing is called process water (Adham et al., 2018b). On average, 3–4 barrels of PW are used for the production of one barrel of extracted oil, and this volume can reach 10 barrels for aged reservoirs (Dores et al., 2012; Munirasu et al., 2016). The global volume of PW was 202 billion barrels in 2014 and was estimated to be approximately 340 billion barrels in 2020 (Dores et al., 2012; Munirasu et al., 2016). The composition of PW can vary from source to source and depends on the extraction method used; however, most PW contains oil in greases (O&G), salts (mainly NaCl), solid particles, polyaromatics, hydrocarbons, and various additives (Neff et al., 2011; Al-Ghouti et al., 2019). The concentration of O&G, which is expressed in terms of

* Corresponding author at: Center for Advanced Materials, Qatar University, P.O. Box 2713, Doha, Qatar.
E-mail address: igor.krupa@qu.edu.qa (I. Krupa).

https://doi.org/10.1016/j.eti.2023.103198
2352-1864/© 2023 The Authors. Published by Elsevier B.V. This is an open access article under the CC BY license (http://creativecommons.org/licenses/by/4.0/).

the total organic carbon content (TOC), ranges from a few tens to a few thousand mg/L (ppm). The treatment of PW cannot be realized with a single process and requires a series of consecutive treatment steps, including primary, secondary, and tertiary treatments that include various mechanical, chemical, physical, and biological methods (Patterson and Patterson, 1985). The tertiary treatment is the final step in water cleaning, and it has a target effluent concentration of <10 mg/L (Pintor et al., 2016). Current tertiary filtration technology typically includes membrane filtration (Dickhout et al., 2017; Padaki et al., 2015; Tanudjaja et al., 2019) and deep bed filtration with activated carbon (Al-Kaabi et al., 2019), synthetic resins (Albatrni et al., 2019), and walnut shells (Rahman, 1992; Yin et al., 2020).

Adsorption is generally considered a very efficient and versatile method for water treatment, and it reduces the contaminant content to very low levels (Dąbrowski, 2001). Adsorption on highly porous media enables the removal of droplets with colloidal dimensions, which cannot be separated by common filtration techniques, such as deep-bed filtration with a walnut shell medium (Rahman, 1992; Yin et al., 2020).

Polymeric foams such as those of cellulose (Abu-Thabit et al., 2022), polydimethylsiloxane (Zhang et al., 2021), polyurethane (Pinto et al., 2018), and melamine (Oliveira et al., 2021; Hailan et al., 2021) are very commonly studied and applied for the removal of free oil from water surfaces. However, foam-based separations of emulsified oil from water mixtures are often limited to the separation of mixtures with relatively high oil contents (over a few volume % and more), simple nonpolar model liquids, and droplet sizes of a few microns and higher (Yang et al., 2019; Han et al., 2020; Zhang et al., 2019).

Melamine foams (MFs) are among the most frequently studied foams because they have highly porous 3D networks (over 99 vol.%), and they exhibit chemical, thermal, and mechanical stability, easy availability, and low cost. Since MFs are inherently oleophilic and hydrophilic, separations of o/w emulsions require modifications resulting in high hydrophobic and oleophilic foams. These modifications involve carbonization (Chen et al., 2013), attachment of graphene (Han et al., 2020) and silica nanoparticles (Li et al., 2015), coating with polydimethylsiloxane (Ong et al., 2019), silanization (Wang et al., 2018), and metal ion complexation (Ding et al., 2018a; Zhang et al., 2020; Dashairya et al., 2020).

Metal ion complexation is a facile fabrication method used for modification of MFs, and it involves immersion in water solutions of suitable salts. This treatment leads to the formation of superhydrophobic and superoleophilic structures, which absorb large amounts of oil, whereas water sorption is neglected. Commercial hydrophilic MFs were immersed in aqueous solutions of transition metal salts (e.g., $FeCl_3$, $Fe(NO_3)_3$, $Zn(NO_3)_2$, $Ni(NO_3)_2$, and $Co(NO_3)_2$) for short periods, followed by drying (Ding et al., 2018a). Highly hydrophobic sponges (with water contact angles of ∼130°) were obtained, and the sponges showed excellent oil absorption capabilities of ca. 71–157 times their weight for a wide range of oils and organic solvents (Ding et al., 2018a). The hydrophilic MFs were transferred into hydrophobic MFs by immersion in a zirconium oxychloride aqueous solution and subsequent drying (Zhang et al., 2020). The modified MFs showed excellent absorption capacities for organic solvents and oils (70–181 g/g) (Zhang et al., 2020). The use of Zr/Cl ions used for polypyrrole (PPy) syntheses led to the preparation of superhydrophobic MFs coated with PPy. They exhibited contact angles of ∼162.6° with a static water droplet and outstanding absorption capacity (∼100–110 g/g) for a wide range of oils and organics solvents (Dashairya et al., 2020).

The present study is focused on the demulsification of colloidal synthetic PW with MFs modified by $FeCl_3$. The effects of media dosage, initial effluent concentration, diffusion and removal kinetics, and reusability of the media were investigated. The Fe^{3+} cations changed the hydrophilic natures of the MFs and made them highly hydrophobic, and they contribute significantly to the adsorption of negatively charged species, such as crude oil droplets modified with an anionic surfactant (sodium dodecyl sulfate). The demulsification mechanism is discussed in detail. To our knowledge, the paper presented here is the first to report successful separations of colloidal oil emulsions comprising droplets with sizes <500 nm that mimic real PW.

1. Materials and methods

1.1. Sorbent media

Commercial melamine foams (MFs) (LTWHOME, Carrefour, Qatar) were washed in distilled water, dried, and cut into $1.5 \times 1.5 \times 1.5$ cm^3 cubes. An aqueous solution of ferric chloride ($FeCl_3$, 97%, Research-Lab Fine Chem Industries, India), with a concentration of 0.01 M was prepared. The MFs were modified via immersion in the ferric chloride solution at room temperature for 30 min with slight shaking. Then, the solution was squeezed out of the foams, and the foams were washed thoroughly with distilled water and dried in a vacuum oven at 60 °C.

1.2. Preparation of synthetic PW

Low-salinity brine was prepared according to a previous report (Dardor et al., 2021), as follows: 1.2 g of sodium chloride (NaCl, 99%), 0.55 g of calcium chloride dihydrate ($CaCl_2 \cdot 2H_2O$, 99%), 0.26 g of magnesium chloride hexahydrate ($MgCl_2 \cdot 6H_2O$, 99%), 0.05 g of potassium chloride (KCl, 99%), 0.035 g of sodium sulfate (Na_2SO_4, 99%, Sigma–Aldrich), 0.015 g of ammonium chloride (NH_4Cl, 99%, Sigma–Aldrich), and 0.07 g of sodium bicarbonate ($NaHCO_3$, 99%, Sigma–Aldrich) were dissolved in 0.5 L of deionized water at 22 °C. In the second step, 30 mg of the surfactant SDS, sodium dodecyl sulfate ($NaC_{12}H_{25}SO_4$, 99%, Riedel-de Haën) and 0.18 mL of crude oil (QP, Qatar) were added to low salinity brine, moderately

stirred for 30 min, and sonicated with a bath sonicator for 30 min. Finally, the synthetic PW was left in a funnel for 24 h to remove the thin oil layer formed at the top of the mixture, and the rest of the emulsion was then used for further tests. This procedure provided synthetic PW containing approximately 100 ppm of total organic carbon (TOC). PW with a lower TOC content was obtained by dilution of the initial PW, whereas PW with a higher TOC was prepared using a higher crude oil content and maintaining a constant crude oil/SDS ratio (Dardor et al., 2021).

1.3. Batch sorption test

The sorption experiments were performed in 50 ml Falcon test tubes. The sizes of the tested foams were arbitrarily chosen to be 1.5 $\times$1.5$\times$ 1.5 cm^3. The number of tested foams varied from 1 to 7 pieces. The test foams were inserted into the tubes, and the tubes were filled with the test emulsions. The sorption experiments were performed at 22 °C for selected periods. The tubes were shaken with a mechanical shaker to avoid the formation of concentration gradients within the emulsions during the experiments. At the end of each test, the foams were removed from the test tubes, and the liquid was squeezed out of the foams one by one by using a syringe to maintain constant conditions for squeezing. The oil contents in the permeate and in the liquid squeezed out of the foam (squeezed permeate) were determined by measuring the total organic carbon (TOC) contents in the samples. The TOC contents for the tested emulsions (batch emulsions) were always remeasured at the beginning of each sorption experiment, and these values were used for subsequent calculations. Each sorption experiment was repeated at least three times.

To determine if the foams could be reused, they were subjected to multiple sorption/desorption experiments. The foams employed for multiple testing (reusage) were used immediately after completing the previous cycle, without any additional cleaning or treatment. This procedure was repeated six times.

1.4. Surface analyses

The morphologies and compositions of the untreated and treated MFs were examined with a Nova NanoSEM 450 (FEI, USA) field emission scanning electron microscope (SEM) equipped with energy dispersive X-ray spectroscopy (EDS), and secondary electron imaging was conducted at 3 kV with different magnifications. All specimens were sputter-coated with a 2 nm thick gold layer before SEM.

Atomic force microscopy (AFM) provided information on the surfaces and topographies/morphologies of the MF foams. An MFP-3D system (Asylum Research, USA) was used to record 3D and 2D AFM images with an AC240TS cantilever and a tip (Al reflex coated Veeco model-OLTESPA, Olympus, Japan). Scanning was performed under air with tapping mode (AC mode) over a surface area of 5 $\times$ 5 μm^2. In addition, the arithmetic average heights of the lines (Ra — roughness parameter) and line profile graphs were obtained from z-Sensor AFM images (piezo crystal response) to generate the most accurate data.

X-ray photoelectron spectroscopy (XPS) was used for characterization of the chemical composition changes induced by modification of MF foams by using iron ions. XPS spectra were captured using an Axis ultra DLD system (Kratos Analytical, UK) containing an Al Ka X-ray source.

1.5. Surface wettability

The surface wettabilities of the foams were characterized by determining the contact angles for distilled water and crude oil with an OCA 35 System (Dataphysics, Germany). The measurements were performed under air and under water for the crude oil.

1.6. Characterization of the emulsions by DLS and zeta potential measurements

A Zetasizer Lab (Malvern Panalytical, UK) was used to determine the droplet sizes by dynamic light scattering (DLS) and the zeta potentials of the emulsions. The DLS measurements were performed in DTS1070 glass cuvettes, and the zeta potentials were determined in ZS90 cuvettes. Each measurement was repeated three times.

1.7. Total organic carbon (TOC) analyses

TOC analyses were performed with a Formacs TOC/TN analyzer (Analytikjena, Germany). The samples were injected into a high-temperature combustion furnace where the organic carbon (OC) was converted to carbon dioxide at 850 °C via catalytic oxidation (Pt catalyst). The formed CO_2 was then dispersed into the carrier gas, and the concentration was measured with a nondispersive infrared detector (NDIR).

1.8. PW morphologies

The distributions of oily droplets within the emulsions were visualized by fluorescence microscopy by using the autofluorescence of the crude oil. One drop of the as-prepared emulsion was applied between microscopic glass slides and analyzed with an EVOS M5000 imaging system. The GFP mode was used for imaging.

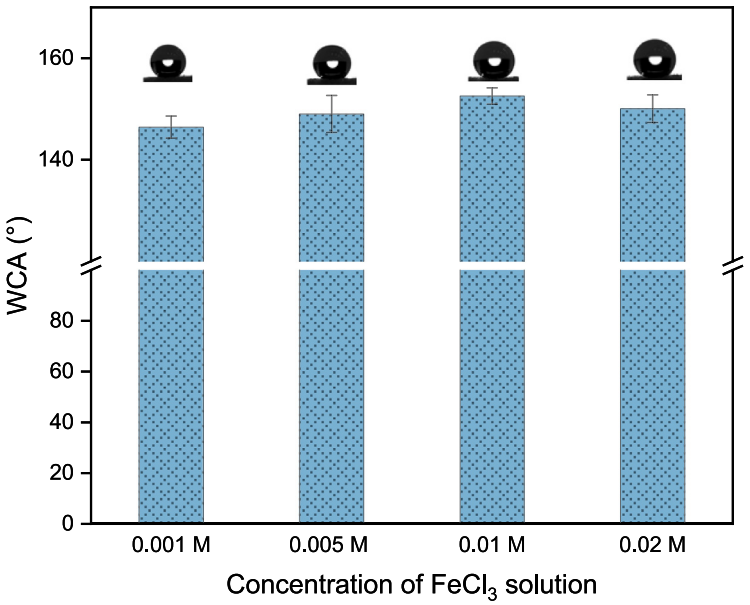

Fig. 1. Water contact angles of modified melamine foams (MFs) with the corresponding images above the bars for the different $FeCl_3$ concentrations.

2. Results and discussion

2.1. Characterization of the unmodified and modified foams

The wettability of unmodified and $FeCl_3$-modified MFs were characterized by measuring the contact angles of water and crude oil in air (for water) and under water (for the crude oil). An unmodified foam showed a CA $< 5°$ and instant penetration of both liquids into the foam structure, indicating superhydrophilicity and oleophilicity of the surface. The modified foams retained the water droplets on their surfaces, which enabled measurement of the water contact angle (WCA). The WCAs for foams modified with 0.01 M solutions were $153 \pm 2°$, which indicated high hydrophobicity of the treated surfaces. The 0.01 M concentration was selected on the basis of preliminary tests. Modification of a foam with $FeCl_3$ dramatically changes its wettability (Ding et al., 2018a). Similar results were also observed for other transition metals (Zhang et al., 2020; Dashairya et al., 2020). Melamine-based foams consist of segments based on 2,4,6-triamino–s triazine rings. In this structure, all the nitrogen atoms have an electron pair, and these form hydrogen bonds and provide hydrophilic polar surfaces. On the other hand, the use of transition metal ions such as ferric (III) ions lead to the formation of strong coordination complexes, and the electron pairs on nitrogen form these complexes. The complexation reduces the abundance of lone electron pairs within the melamine structure, which also increases the planarity of melamine structures in the network. Based on these factors, the modified melamine structure made the surface superhydrophobic.

The MFs were modified with solutions containing different concentrations of $FeCl_3$, and the water contact angles are shown in Fig. 1.

The SEM micrographs (Fig. 2A, B) showed insignificant MFs morphology changes after modification, maintaining large fully opened pores within a network comprising fibers with thicknesses of 6 ± 3 μm. EDS maps (Fig. 2C, D) were generated for the cross-sections of the modified MFs and revealed even distributions of the Fe elements within the fibrous network structures. The weight contents for the detected atoms were: $32.8 \pm 1.4\%$ for C, $41.6 \pm 1.7\%$ for N, $13.6 \pm 1.9\%$ for O, $5.4 \pm 0.1\%$ for Fe, and $5.1 \pm 0.1\%$ for Cl.

Complexation of the Fe was confirmed with XPS. High-resolution Fe 2p and Cl 2p XPS spectra showed that both were contained in the modified sample, while they were absent from the unmodified sample (Fig. 3).

The detailed surface topographies of unmodified and modified MFs were determined with AFM over a 5×5 μm^2 surface area, and the AFM images are shown in Fig. 4. The surface topography/morphology of the unmodified MFs revealed a rough but uniform structure. The roughness parameter Ra value exhibited a value of 5.9 nm (Fig. 4A). Modification of a MF with the $FeCl_3$ solution led to rougher structures in the top surface of the MFs and an Ra value of 119.3 nm. These structural changes indicated successful surface modification of the MFs at the micro level.

The densities of the untreated and treated MFs were determined from their masses and volumes before and after treatment. The densities of the pristine and treated MFs were $(8.07 \pm 0.15) \times 10^{-3}$ g cm^{-3} and $(10.26 \pm 0.19) \times 10^{-3}$ g cm^{-3}, respectively. The porosities of the foams (ϕ_p) were estimated with Eq. (1):

$$\phi_p\,(\%) = \left(1 - \frac{\rho_f}{\varrho_m}\right) \times 100\% \tag{1}$$

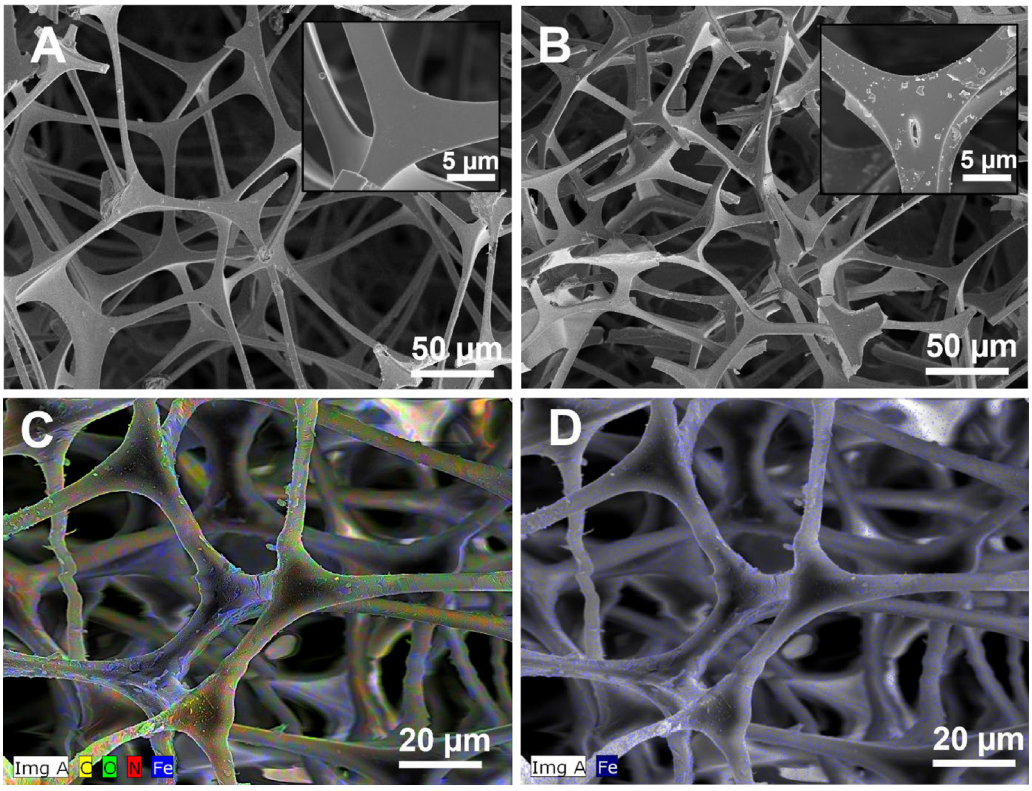

Fig. 2. SEM micrographs of pristine MFs (A) and treated MFs (B); EDS maps for C, O, N and Fe in a treated MFs (C) and EDS map for Fe in a treated MFs (D).

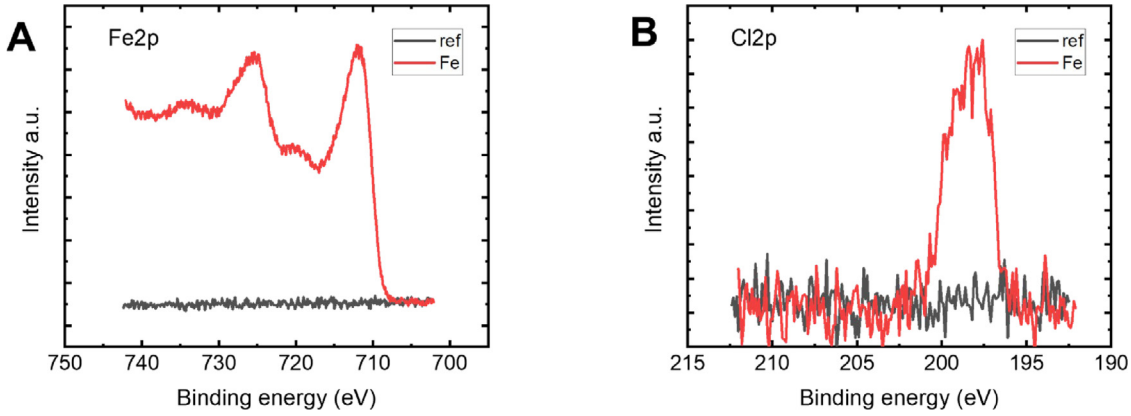

Fig. 3. (A) Fe 2p and (B) Cl 2p XPS data for an untreated MFs (ref) and a treated MFs (Fe).

where the density of the solid melamine resin was $\rho_m = 1.51$ g cm^{-3} (Ding et al., 2018a; Ritger and Peppas, 1987b). The porosities of the pristine and treated MF were 99.5 vol,% and 99.3 vol.%, respectively. The specific surface area of an untreated MA foam with a similar porosity was approximately 70 m^2/g (Stejskal et al., 2022).

2.2. Characterization of the synthetic PW

The droplet size distribution for the as-prepared PW (carbon content of 120 ± 5 ppm) was characterized with dynamic light scattering. The differential distribution curve was determined from measurements of five independently prepared emulsions. The emulsion contained 63 vol.% for droplets with dimensions below 500 nm and 90 vol.% for droplets with sizes below 1000 nm, and the modal diameter (the diameter at the peak) was 468 ± 35 nm, which confirmed the colloidal

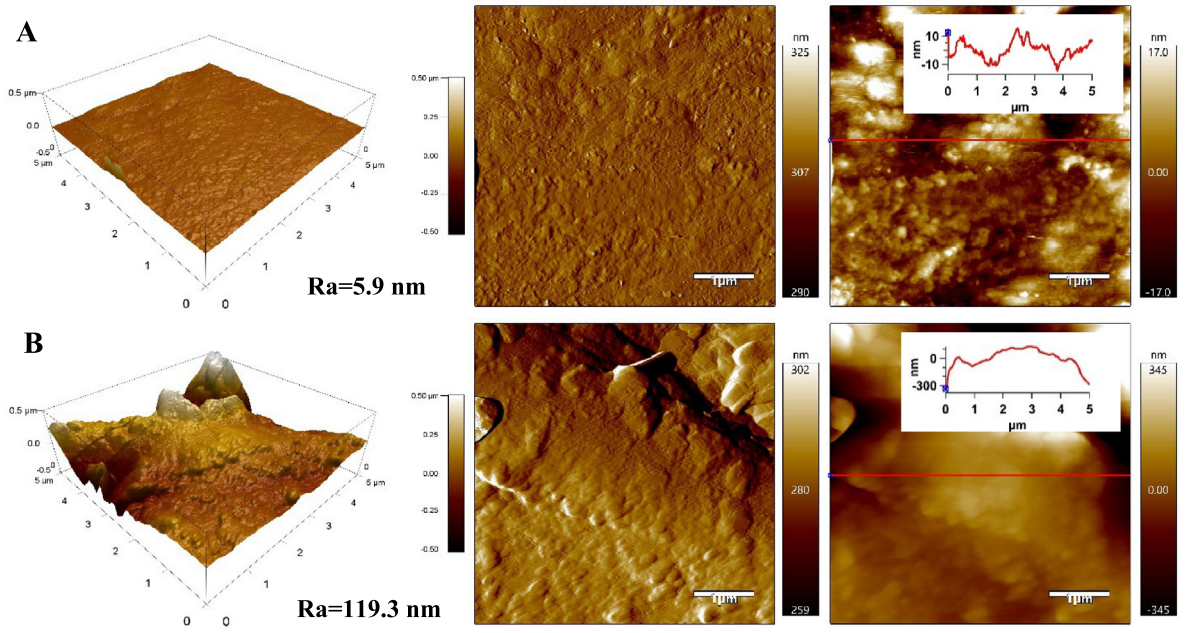

Fig. 4. AFM images (3D height, 2D amplitude, 2D z-sensor with line profile graph) of an unmodified MFs (A) and a modified MFs (B).

character of this emulsion. The residual oil formed large aggregates with sizes of 5–6 μm. The zeta potential of the PW was −54.0 mV, which indicated good kinetic stability of the emulsions due to the anionic surfactants. Various theoretical and empirical functions have been used to describe droplet size distributions. They involve the Gauss normal distribution function, log-normal distribution, Rosin–Rammler equation, Nukiyama–Tanasawa equation, and others (Jurado et al., 2007). The Nukiyama–Tanasawa equation (Hrubecky, 1958) was arbitrarily used after rewriting its original form, as shown in Eq. (2):

$$f_{nl}\,(d_i) = K\delta^n \exp(-k\delta^m) \tag{2}$$

where f_{nl} is the droplet size distribution function, δ is the dimensionless diameter, and K, n, k, and m are empirical parameters. The simplified distribution function (f(x)) used for fitting the experimental data is given by Eq. (3a):

$$f\,(x) = Axexp(-Bx^2) \tag{3a}$$

where x is the droplet size/diameter [nm], and A and B are adjustable parameters.

The meaning of parameter B was determined by differentiating the equation; $\left(\frac{df}{dx}\right)_{x=x_o} = 0$ (resulting in $B = 1/2x_0^2$).

Then, the distribution function f(x) can be expressed by Eq. (3b):

$$f\,(x) = Axexp(-\frac{x^2}{2x_0^2}) \tag{3b}$$

where x_0 is the modal diameter. The parameters obtained by fitting the experimental data were $A = 2.7 \times 10^{-2} \pm 5.8 \times 10^{-4}$ [nm^{-1}] and $B = 2.1 \times 10^{-6} \pm 8.4 \times 10^{-8}$ [nm^2]. Parameter B gives the modal diameter $x_0 = 491$ nm (see Fig. 5).

The PW emulsions were also analyzed with fluorescence microscopy. No additional fluorescence probe was used because crude oil exhibits autofluorescence. Oil droplets with various sizes ranging from the submicron range to a few tens of microns are visible in Fig. 6, indicating good homogeneity of the emulsion and the absence of large aggregates.

2.3. Demulsification of the PW

(i.) Diffusion of the PW into modified MFs

Treatment of the MFs led to the formation of (super)hydrophobic surfaces, as discussed previously. Superhydrophobicity is a consequence of the chemical composition ensuring a low surface energy for the skeleton material and a surface topology with an appropriate roughness, and it can be explained and described with the Wenzel model (Wenzel, 1936) or the Cassie–Baxter model (Cassie and Baxter, 1944). However, in some cases, the hydrophobicity may not suppress the

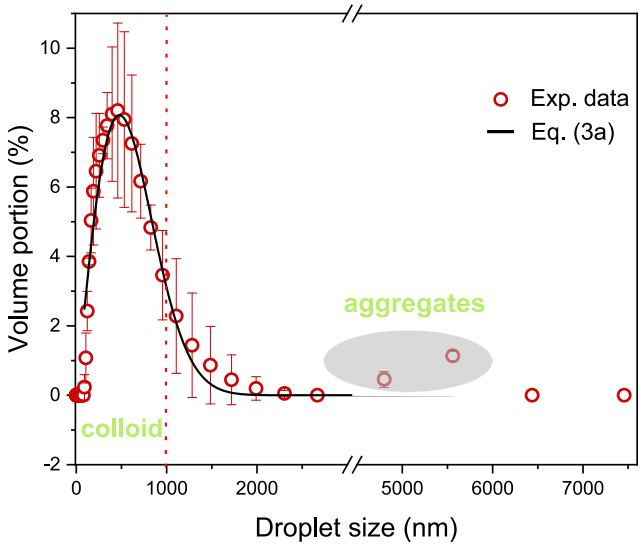

Fig. 5. Droplet size distribution curve.

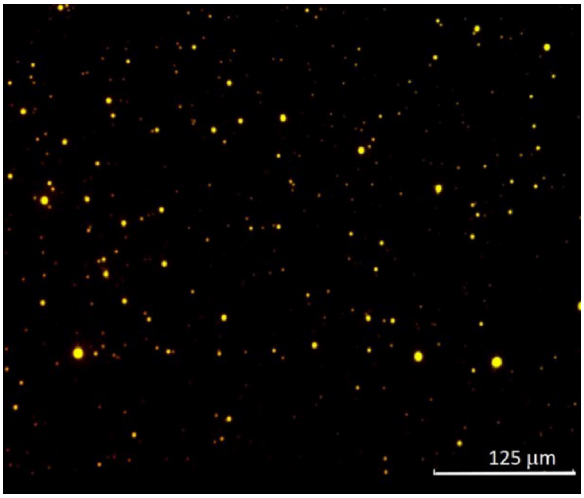

Fig. 6. Fluorescence image of the PW.

diffusion of water (or emulsions) into the foam, particularly if it is immersed in water, the system is shaken or stirred, or the water exposure time is sufficiently long. In this case, the pores or voids on the material surface, which are initially filled by air, can be filled with water, and then the liquid penetrates the foam. However, chemical modification of the foam leads to significantly reduced water diffusion over the whole volume. In other words, the hydrophobicity induced by the Fe^{3+} cations still plays a role. This phenomenon is crucial for the separation of oil emulsions by foamy structures. Fig. 7a and b show amounts of PW absorbed within a treated foam (1.5 ×1.5× 1.5) cm^3 over a long time interval (Fig. 7a) and a short time interval (Fig. 7b). It was also observed that the amount of PW adsorbed by a foam floating on the PW surface was negligible.

Fig. 3a shows that the foam was fully saturated by liquid approximately 40 min after immersion. The time required for foam saturation depended on the size and shape of the foam, as shown by the general theory of diffusion (Ritger and Peppas, 1987a,b). The sizes and shapes of the tested foams were arbitrarily chosen, and all of the foams used in this study had the same shapes and sizes.

The kinetics for PW sorption at the early stage (short times) can be described with a linear function (Eq. (4)):

$$W(t) = At \tag{4}$$

where A $[s^{-1}] = 1.12 \pm 0.02$ $[s^{-1}]$ and $R^2 = 0.9951$.

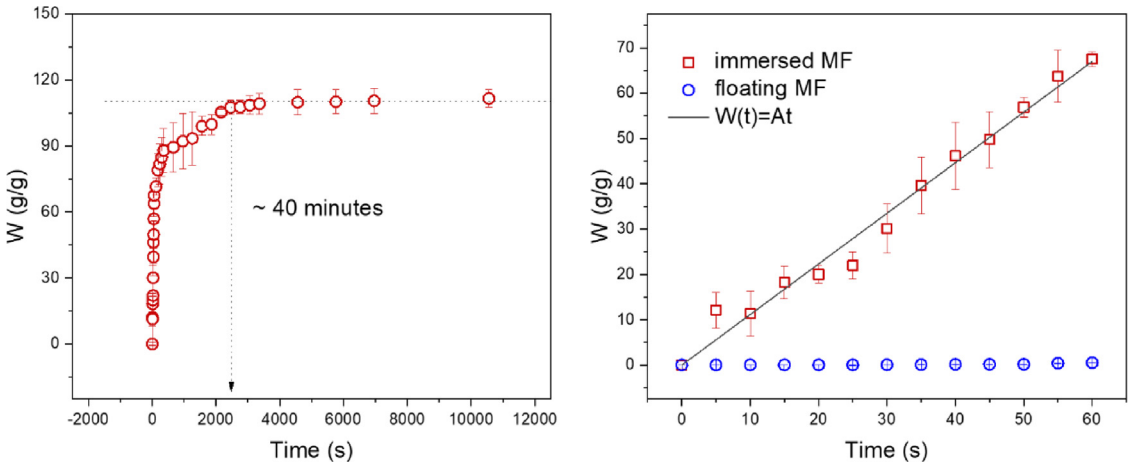

Fig. 7. Time dependence for PW sorption into a treated MFs (1.5 × 1.5 × 1.5 cm^3); (a) full-time scale and (b) short time scale.

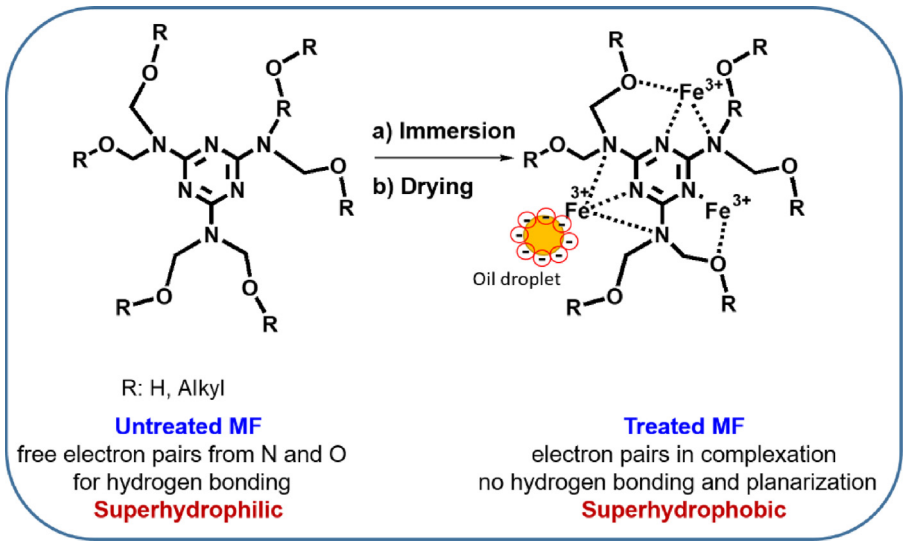

Fig. 8. Sketch indicating oil droplet separation with treated MFs.

The diffusion of an emulsion into a foam is crucial for demulsification by foamy structures. The major phase is water, which acts as a carrier for the oil droplets that transport the molecules into the internal structure of the foam. The effect of Fe^{3+}on the separation efficiencies of modified MFs is not primarily based on the induced hydrophobicity/oleophilicity of the structure, since this only alters the diffusion rate into the foam. The key phenomenon is selective adsorption of the negatively charged oil droplets on the internal surfaces of the foam (a solid skeleton), which are at least partially positively charged. The mechanism for separation of the charged oil droplets is shown in Fig. 8.

(ii.) Effect of the foam dosage

It is generally known that the separation efficiencies of sorbents depend on the ratio of the sorbent dosage and the volume of the treated emulsion (Pintor et al., 2016). The amount of sorbent is usually (for practical reasons) expressed in mass units, but it can also be expressed in volumetric units. In the following text, ratios of foam volumes and treated emulsion volumes are considered, and the foam volumes are arbitrarily expressed by the number of foam cubes used. If relevant, the sorption parameters are related to the masses of the foams. The volume and size of each foam were always constant (1.5 × 1.5 × 1.5 cm^3), the masses were 0.027 ± 0.001 g, and the volumes of the treated emulsions were equal to the volumes of the test tubes (50 mL). From a practical standpoint, the dimensions of the foams were arbitrarily selected to simplify the manipulation.

In the first stage, the dosage (the number of cubes) was optimized for further testing. For this reason, multiple experiments were performed to test PW removal from a 120 ppm emulsion within 24 h, and 1, 3, 5, or 7 modified foam cubes were used.

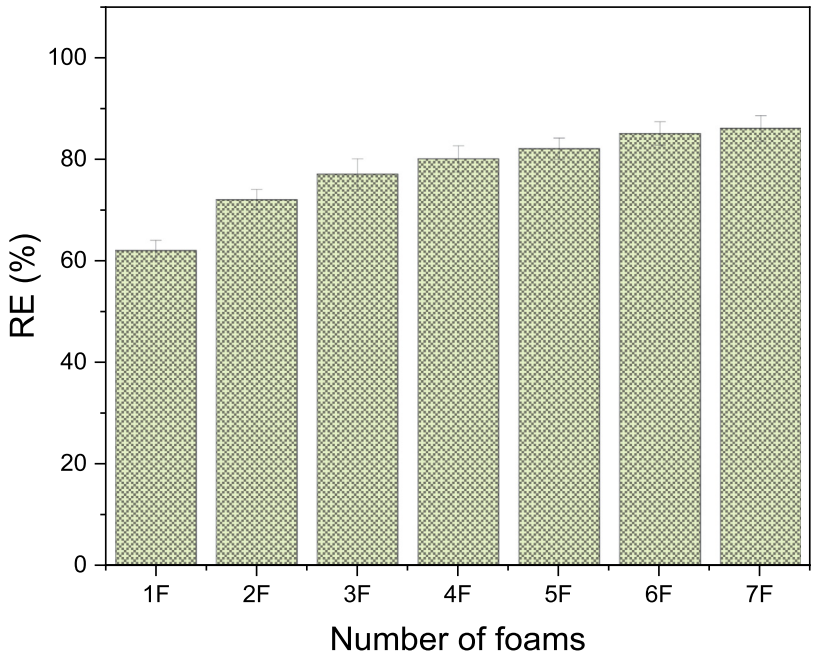

Fig. 9. Dependence of the removal efficiency on the number of foam cubes used.

As expected, more foam cubes enhance the sorption efficiency up to some limit, which was 86 ± 3% for 7 foam cubes (Fig. 9). The addition of more foam cubes did not lead to further improvement in the sorption efficiency, and therefore, seven foams were used for all further sorption experiments.

Recalculation of the '*ad hoc*' defined dosage to a dosage expressed in mass units [g] was performed by using the foam density $(10.26 \pm 0.19)\times10^{-3}$ g cm^{-3}.

For comparison, seven untreated MF cubes were tested under the same conditions, and the separation efficiency was approximately 7%.

(iii.) Effect of the initial crude oil concentration

Absorption experiments were performed at 22 °C and for 24 h with seven foam cubes immersed in 50 mL emulsions containing different crude oil contents. The concentrations chosen for these experiments were related to the concentration range for oil impurities in the produced water; this is characteristic of the tertiary and secondary treatments of emulsified water and the range is 40 to 200 ppm of carbon in the emulsion. The total carbon content, which is the experimentally determined parameter, includes contributions from both the crude oil and the surfactant (SDS).

The adsorption capacity (q_e) is an important parameter used to characterize the adsorption process, and it is defined as the mass of adsorbed species (oil) per mass of the adsorbent (MFs). This parameter is commonly calculated from the difference between the initial (c_0) and equilibrium (c_e) liquid phase concentrations of the dissolved oil particles or other investigated species. This approach is not directly applicable for foamy, porous sorbents because they absorb a significant amount of the emulsion and not only the oil droplets; also, after removal of the emulsion by squeezing, some of the liquid remains inside the foam. Determination of the carbon content in the filtrate (permeate) is not sufficient to differentiate the oil content within the foam, which belongs to the residual emulsion, and the oil adsorbed onto the solid skeleton. The volume of residual liquid within a foam is not negligible and represents approximately 8–10% of the total absorbed liquid. Moreover, if a large amount of surfactant is used, the carbon content of the surfactant contributes to the total organic carbon content measured. Herein, we propose a method for estimating the amount of oil adsorbed on a solid foam skeleton with some easily experimentally determined parameters. All these parameters can be obtained from a single sorption experiment and must be determined with high accuracy (see Table 1).

The next factors are based on the emulsion mass balance and the total carbon mass balance in the foam before and after squeezing. As mentioned above, the foam contains three components (oil, surfactant, and water) after squeezing and three phases (oil/surfactant structure adsorbed on the skeleton, oil/surfactant phase dispersed in water, and water). The carbon content in this phase depends on the chemical compositions of the oil and surfactant as well as on their mass ratio in the emulsion, which will be discussed later. The presence of free surfactant is not considered. The material balance for the emulsion and the carbon in the squeezed foam is described by Eqs. (5a), (5b), (5c):

$$m_{a,o} + m_{f,o} + m_w = M_1 \tag{5a}$$

Table 1
Parameters used for calculating the $q_e = f(c_0)$ dependence.

Parameter/Units	Description
m_F (g)	Mass of the neat foam
$m_{e,0}$ (g)	Mass of the initial emulsion
$TOC_{em,0}$ (mg/kg)	Concentration of carbon in the initial emulsion (carbon from both the oil and surfactant)
m_F^{sat} (g)	Mass of the foam saturated by emulsion (at the end of the experiment)
m_F^{sq} (g)	Mass of the foam after squeezing the liquid out
m_{em}^{sq} (g)	Mass of the squeezed liquid
m_{em}^{filt} (g)	Mass of the filtrate (residual emulsion at the end of the experiment)
TOC^{filt} (mg/kg)	Concentration of carbon in the filtrate
TOC^{sq} (mg/kg)	Concentration of carbon in the liquid squeezed out from the foam

$$xm_{a,o} + xm_{f,o} = M_2 \tag{5b}$$

$$\frac{xm_{f,o}}{xm_{f,o} + m_w} = TOC^F \equiv TOC^{sq} \tag{5c}$$

where $m_{a,o}$ is the mass of the oil adsorbed on the skeleton, $m_{f,o}$ is the mass of the oil in the emulsion within the foam after squeezing, and m_w is the mass of the water in the emulsion within the foam after squeezing. The term 'water' refers to water and the dissolved salts (also called brine), except for the oil and surfactants.

M_1 and M_2 are calculated from Eqs. (6a), (6b):

$$M_1 = m_F^{sq} - m_F \tag{6a}$$

$$M_2 = m_{em,o}TOC_{em,o} - m^{filt}TOC^{filt} - m_{em}^{sq}TOC^{sq} \tag{6b}$$

Parameter x characterizes the weight portion of the carbon in the oil/surfactant phase, and it will be determined later.

Eq. (5c) gives the carbon content of the residual emulsion remaining in the foam after squeezing (TOC^F). This value is not directly measurable; however, it is reasonable to assume that this value is equal to the concentration of carbon in the liquid that is squeezed out from the foam — TOC^{sq}. In this case, Eqs. (5a), (5b), (5c), including the three independent variables ($m_{a,o}$, $m_{f,o}$, m_w) and one parameter x, enable the calculation of $m_{a,o}$ with Eq. (7):

$$m_{a,o} = \frac{M_2 - xAM_1}{x(1-A)}; \quad A = \frac{TOC^{sq}}{TOC^{sq} + x(1 - TOC^{sq})} \tag{7}$$

Finally, q_e is determined from Eq. (8):

$$q_e = \frac{m_{a,o}}{m_F} \tag{8}$$

The last step is the determination of parameter x, which represents the weight fraction of carbon in the oil/surfactant system. This parameter is calculated from the following data:

(i.) The mass ratio of oil and surfactant in the emulsion. According to the protocol (Dardor et al., 2021) used in this study, this ratio is related to the oil and surfactant portions: 0.18 g for the oil and 30 mg for the surfactant (sodium dodecyl sulfate).
(ii.) The density of the crude oil is 0.875 g cm^{-3}.
(iii.) The weight portion of the carbon in the crude oil is 0.85 (determined by elemental analysis).
(iv.) The weight portion of the carbon in the surfactant is 0.5 (M = 288.38 g mol^{-1}).

From these data and considering that the total amount of surfactant is consumed in covering the oil droplets (i.e., there is no free surfactant in the emulsion), the value of x is 0.794.

The experimental data used to calculate q_e for different initial concentrations of oil (c_0) are shown in Table 2.

The dependence of q_e on the initial concentration of oil (c_0) is shown in Fig. 10 and can be determined from Eq. (7):

$$q_e = Kc_0 \tag{9}$$

where $K = 0.2307 \pm 0.0071$ [$(mg/g)^{-1}$], and $R^2 = 0.99402$.

For similar oil initial concentrations (a few tens of mg/g), the q_e values are comparable to the adsorption capacities determined by Albatrni et al. (2019) for commercial synthetic resins such as Optipore L493, Amberlite XAD 7, and Lewatit AF 5, which are commonly used as polymeric adsorbents to remove oil from water. Moreover, the modified MFs showed significantly higher sorption capacities for higher initial concentrations of oil.

(iv.) Kinetics of oil (carbon) removal from PW

Table 2
Experimental data used to determine q_e.

Parameter	200 ppm	160 ppm	120 ppm	90 ppm	40 ppm
Mass of the neat foam, m_F (g)	0.2278	0.2152	0.2204	0.2222	0.2261
Stock concentration, $TOC_{em,0}$ (mg/kg)	198	155	117	87	39
Mass of the treated emulsion, $m_{em,0}$ (g)	49.371	49.013	49.042	48.903	49.861
Mass of the saturated foam, m_F^{sat} (g)	23.317	21.083	21.719	21.3012	21.420
Mass of the filtrate, m^{filt} (g)	25.658	27.812	27.163	27.602	27.482
Mass of the squeezed liquid, m_{em}^{sq} (g)	21.019	19.029	18.371	19.485	18.912
Mass of the squeezed foam, m_F^{sq} foams (g)	2.187	1.906	3.223	1.675	2.407
TOC of the filtrate, TOC^{filt} (mg/kg)	35	22	16	29	13
TOC of the squeezed liquid, TOC^{sq} (mg/kg)	34	22	16	27	13
Removal efficiency (%)	83	85	86	66	67

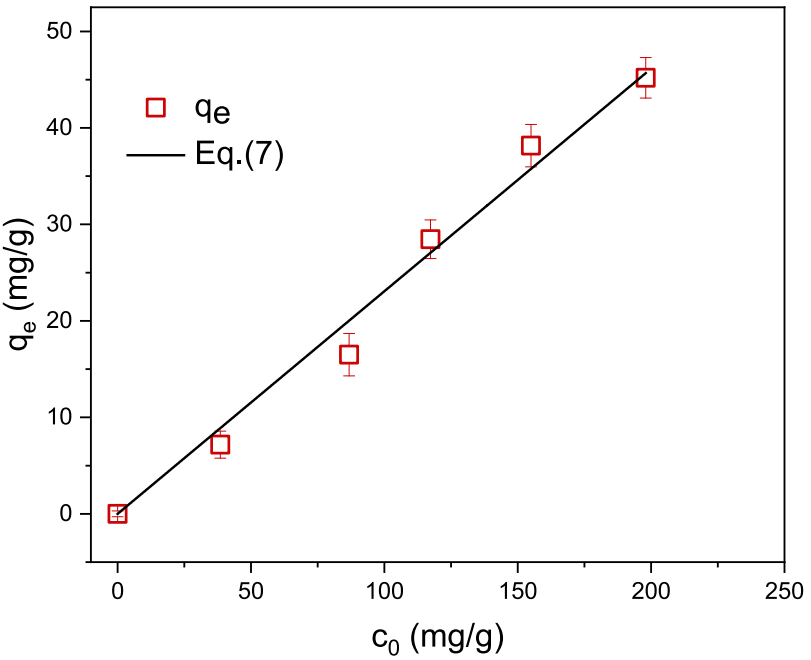

Fig. 10. Dependence of the adsorption capacity (q_e) on the initial concentration of oil (expressed as the total organic carbon content).

Absorption experiments were performed by immersing seven foam cubes in 50 mL of 120 ppm PW at 22 °C and for various sorption times ranging from zero to 24 h.

The time-dependent sorption capacity (S_w) for the foam is expressed by Eq. (10):

$$S_w(t) = \frac{c_0 - c(t)}{m_{0,f}} V \tag{10}$$

where c_0 [mg/L] is the initial concentration of oil in the emulsion, c(t) is the concentration of oil in the emulsion at time t, V [mL] is the volume of the emulsion to be analyzed, and $m_{0,f}$ [mg] is the initial weight of the neat foam. At equilibrium (in the limit as $t\to\infty$), the concentration of oil in the emulsion is $c(t\to\infty)$, and the limiting sorption capacity (S_w^{∞}) is given by Eq. (11):

$$S_w^{\infty} = \frac{c_0 - c(t \to \infty)}{m_{0,f}} V \tag{11}$$

The removal efficiency (RE) is commonly used for characterizing the sorption process, and it is defined as in Eq. (12):

$$RE(t)[\%] = \frac{c_0 - c(t)}{c_0} \times 100\%; \quad RE^{\infty}[\%] = \frac{c_0 - c(t \to \infty)}{c_0} \times 100\% \tag{12}$$

The experimental dependence of the removal efficiency (RE) (defined as in Eq. (12)) on time is shown in Fig. 11.

The sorption process can be roughly divided into two stages. In the first stage, diffusion of the emulsion into the foam is the dominant process. It is accomplished by simultaneous diffusion of oil droplets into the foam and adsorption

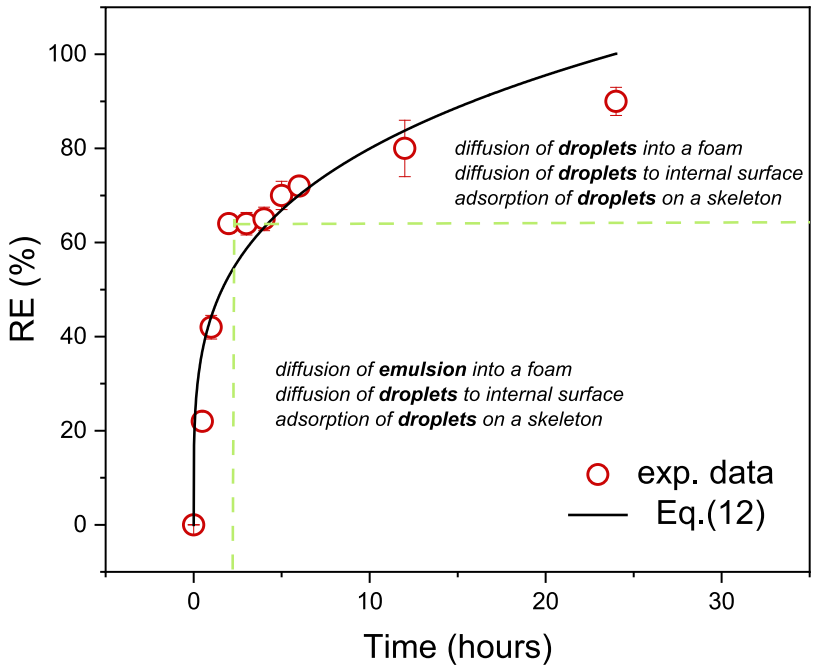

Fig. 11. Dependence of the removal efficiency (RE) on time.

of the oil droplets on the internal surfaces (fibers) of the foam. In the second stage, when the foam is fully saturated, oily droplets inside the foam continuously diffuse to the fibers and adsorb onto the internal surfaces of the foam. This leads to a decrease in the local oil concentration within the foam and generation of a concentration gradient for the emulsion inside and outside the foam. This causes additional transport (diffusion) of oil droplets from the emulsion to the foam. These processes are dominant for approximately two hours, and during this period, approximately 64% of the oil is removed. After this time, the rate for removal of the oil from the emulsion starts to decelerate significantly. With increasing time, the rate for oil adsorption on the MF skeleton decreases, and thus, less oil diffuses from the emulsion to the foam; therefore, the removal efficiency decreases. Finally, when the rate for adsorption of oil droplets onto the fibers is very low, the concentrations inside and outside the foam are close to equilibrium, and the process for oil removal from the emulsion stops. In this study, the duration for the entire experiment was arbitrarily chosen as 24 h because continuation of the process beyond this time had a negligible effect on the removal efficiency. The removal efficiency after 24 h was approximately 86 ± 3%.

The most common models used to describe the adsorption of low molar mass species from liquids (mostly water) are the pseudo-first-order model (PFOM) (Hossain et al., 1898), the pseudo-second-order model (PSOM) (Ho and McKay, 1998), and the Weber–Morris intra-particle diffusion model (IPD) (Weber and Morris, 1963). In some cases, but not always, these models are also useful in characterizing the absorption processes, as discussed by Khosravi and Azizian (2016). An analysis showed that neither the PFOM nor PSOM fit the experimental data sufficiently. The Weber-Morris intraparticle diffusion model (IPD) is most frequently applied to systems in which adsorption is accomplished by diffusion; however, this model also did not fit the data well because of the non-Fickian character of sorption, as discussed above.

A more general approach for describing diffusional processes is the generalized non-Fickian diffusional model, given by Eq. (13), which was originally introduced by Ritger and Peppas (1987a,b) for the interpretation of non-Fickian drug release from moderately swelling polymeric systems.

$$\frac{M_t}{M_\infty} = kt^n \tag{13}$$

In the original papers, M_t and M_∞ were the mass concentrations of the released species at time t, and at a time approaching infinity, k was a constant characteristic of the network (medium) and the species, and n was a diffusional exponent. This model is broadly applied in describing diffusion-controlled release of substances from solid media and diffusion of substances from liquids to solid media. Additionally, another quantity instead of the parameters M_t and M_∞ can be used to characterize the sorption process, such as, the removal efficiency (RE, RE^∞) defined in Eq. (12). In this case, the non-Fickian diffusional model (Eq. (13)) can be rewritten as in Eq. (14) after simple algebraic manipulations:

$$\frac{RE(t)}{RE^\infty} = kt^n \tag{14}$$

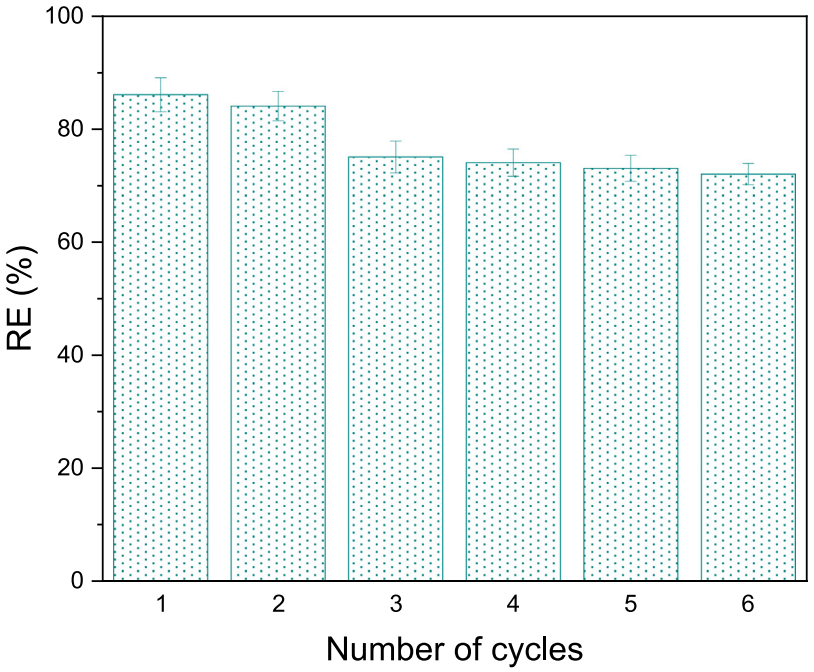

Fig. 12. MF removal efficiencies (REs) for six consecutive cycles.

Fig. 11 shows that this model gave a good fit to the experimental data. The fitting function used had the general form $RE(t) = At^n$ ($A = RE^{\infty}k$), and the following parameters were obtained: A= 17.0 ± 2.0 [% min^{-n}], n = 0.24 ± 0.02 [–], and R = 0.99399. The parameter n was significantly smaller than 0.5, indicating a strongly non-Fickian diffusion.

Control adsorption experiments were performed with unmodified MFs and various initial oil concentrations. The unmodified MFs did not separate these oil emulsions at all, regardless of the initial oil concentration and the duration of the experiment. In other words, the carbon contents (TOC value) in the emulsions at the beginning of the experiments were the same as those in the emulsions at the end of the experiments. Additionally, the carbon content determined for the emulsion at the end of the experiment was the same as the carbon content in the emulsion squeezed out of the foam (within experimental error). This clearly confirmed that the unmodified MFs did not adsorb oil droplets on their skeleton surfaces.

(v.) Reusability of the foams

Regeneration and reusability of the sorbents are important for practical use in wastewater treatment (Saleem et al., 2021). For the case of foamy sorbents, the easiest method for sorbent recovery was simple squeezing, which was most appropriate for foam recovery after the sorption of neat oils (Pintor et al., 2016; Hailan et al., 2021). On the other hand, if the adsorption sites are saturated and adsorption cannot proceed, regeneration of the sorbents by various thermal, chemical, and microbiological methods must be applied (Salvador et al., 2015a,b). In this study, only the simple squeezing MFs regeneration method was tested. For this reason, ten consecutive sorption–desorption cycles were performed with an emulsion containing 120 ppm of total organic carbon and seven foam cubes. The duration for each cycle was 4 h. The foams used in the *i*th cycle were also used in the (i−1)th cycle; only the liquid was squeezed out, and no additional drying or cleaning step was performed. The MFs removal efficiencies for the six cycles are shown in Fig. 12.

It was found that the efficiencies of the foams decreased slightly with increasing numbers of cycles due to absorbed oil on the foam skeleton that could not be removed by simple squeezing of the sponge. It is also noteworthy that the simple squeezing method used in this study cannot be used to remove all of the liquid from the foam. The mass of the foams was 0.191 ± 0.004 g, the mass of the absorbed liquid was 17.4 ± 0.6 g, and the mass of the permanently trapped liquid was 1.37 ± 0.08 g; thus, the trapped liquid remaining after squeezing represented approximately 8% of the absorbed liquid. On the other hand, the trapped liquid content did not increase with increasing numbers of cycles and remained more or less constant.

3. Conclusions

This study addressed the demulsification of synthetic produced water with melamine foams modified by ferric chloride. This is the first study demonstrating the use of a modified MF foam for efficient demulsification of low-concentration colloidal emulsions mimicking actual produced water. The Fe^{3+} cations not only changed the hydrophilic character of the

foams and made them highly hydrophobic, it also contributed significantly to the adsorption of negatively charged species, such as droplets of crude oil modified with an anionic surfactant (sodium dodecyl sulfate). Modified melamine foams, despite their hydrophobicities in air, which were demonstrated with water contact angle measurements, also enabled gradual diffusion of the PW into the internal structure of the foam, which is important for the transfer of oily droplets into the foam. The demulsification mechanism involved multiple diffusion processes running at different time scales, including diffusion of the emulsion into the foam, diffusion of the oil droplets within the foam, and diffusion of the individual oil droplets into the foam and simultaneous adsorption of oil droplets onto the solid skeleton of the foam. The adsorption capacity (q_e) increased linearly with increases in the initial concentration of organic carbon originating from the crude oil and the surfactant over the concentration range 40 to 200 ppm. A simple procedure was proposed for determining the adsorption capacity of a MFs. The MF removal efficiency for emulsions containing carbon contents above 100 ppm was approximately 86%. The multiple reuses of foam cubes was also demonstrated.

This study indicated that melamine foams treated with $FeCl_3$ provided a simple and inexpensive method for treating emulsified produced water containing colloidal oily impurities, particularly with a batch configuration.

CRediT authorship contribution statement

Sarah Hailan: Data curation, Formal analysis, Writing – original draft. **Patrik Sobolciak:** Formal analysis, Supervision, Writing – review & editing. **Peter Kasak:** Methodology, Writing – review & editing. **Anton Popelka:** Methodology, Writing – review & editing, Formal analysis. **Yongfeng Tong:** Data curation, Formal analysis. **Samer Adham:** Resources, Writing – review & editing. **Igor Krupa:** Conceptualization, Project administration, Supervision, Validation, Writing – original draft, Writing – review & editing.

Declaration of competing interest

The authors declare that they have no known competing financial interests or personal relationships that could have appeared to influence the work reported in this paper.

Data availability

Data will be made available on request.

Acknowledgments

The FESEM measurements of the samples were performed in the Central Laboratories Unit at Qatar University. The fluorescence image of the PW was obtained at the Biomedical Research Center, Qatar University. The Core Labs at Hamad Bin Khalifa University are acknowledged for XPS measurements. All authors approved the version of the manuscript to be published. Open access funding was provided by the Qatar National Library.

Funding

This research was made possible by a grant from the Qatar National Research Fund under its National Priorities Research Program (award number NPRP12S-0311-190299) and by financial support from the ConocoPhillips Global Water Sustainability Center (GWSC), Qatar and Qatar Petrochemical Company (QAPCO). The paper's content is solely the responsibility of the authors and does not necessarily represent the official views of the Qatar National Research Fund or ConocoPhillips and QAPCO.

References

Abu-Thabit, N.Y., Uwaezuoke, O.J., Abu Elella, M.H., 2022. Superhydrophobic nanohybrid sponges for separation of oil/ water mixtures. Chemosphere 294, http://dx.doi.org/10.1016/J.CHEMOSPHERE.2022.133644.

Adham, S., Hussain, A., Minier-Matar, J., Janson, A., Sharma, R., 2018a. Membrane applications and opportunities for water management in the oil & gas industry. Desalination http://dx.doi.org/10.1016/j.desal.2018.01.030.

Adham, S., Hussain, A., Minier-Matar, J., Janson, A., Sharma, R., 2018b. Membrane applications and opportunities for water management in the oil & gas industry. Desalination 440, 2–17. http://dx.doi.org/10.1016/j.desal.2018.01.030.

Al-Ghouti, M.A., Al-Kaabi, M.A., Ashfaq, M.Y., Da'na, D.A., 2019. Produced water characteristics, treatment and reuse: A review. J. Water Process Eng. 28, 222–239. http://dx.doi.org/10.1016/J.JWPE.2019.02.001.

Al-Kaabi, M.A., Al-Ghouti, M.A., Ashfaq, M.Y.M., Ahmed, T., Zouari, N., 2019. An integrated approach for produced water treatment using microemulsions modified activated carbon. J. Water Process Eng. 31, 100830. http://dx.doi.org/10.1016/j.jwpe.2019.100830.

Albatrni, H., Qiblawey, H., Almomani, F., Adham, S., Khraisheh, M., 2019. Polymeric adsorbents for oil removal from water. Chemosphere 233, 809–817. http://dx.doi.org/10.1016/j.chemosphere.2019.05.263.

Cassie, A.B.D., Baxter, S., 1944. Wettability of porous surfaces. Trans. Faraday Soc. 40 (546), http://dx.doi.org/10.1039/tf9444000546.

Chen, S., He, G., Hu, H., Jin, S., Zhou, Y., He, Y., He, S., Zhao, F., Hou, H., 2013. Elastic carbon foam via direct carbonization of polymer foam for flexible electrodes and organic chemical absorption. Energy Environ. Sci. 6 (2435), http://dx.doi.org/10.1039/c3ee41436a.

Dąbrowski, A., 2001. Adsorption — from theory to practice. Adv. Colloid Interface Sci. 93, 135–224. http://dx.doi.org/10.1016/S0001-8686(00)00082-8.

Dardor, D., Al-Maas, M., Minier-Matar, J., Janson, A., Sharma, R., Hassan, M.K., Al-Maadeed, M.A.A., Adham, S., 2021. Protocol for preparing synthetic solutions mimicking produced water from oil and gas operations. ACS Omega 6, 6881–6892. http://dx.doi.org/10.1021/acsomega.0c06065.
Dashairya, L., M, G., Saha, P., 2020. Synergistic effect of Zr/Cl dual-ions mediated pyrrole polymerization and development of superhydrophobic melamine sponges for oil/water separation. Colloids Surf. A 599, 124877. http://dx.doi.org/10.1016/J.COLSURFA.2020.124877.
Dickhout, J.M., Moreno, J., Biesheuvel, P.M., Boels, L., Lammertink, R.G.H., de Vos, W.M., 2017. Produced water treatment by membranes: A review from a colloidal perspective. J. Colloid Interface Sci. http://dx.doi.org/10.1016/j.jcis.2016.10.013.
Ding, Y., Xu, W., Yu, Y., Hou, H., Zhu, Z., 2018a. One-step preparation of highly hydrophobic and oleophilic melamine sponges via metal-ion-induced wettability transition. ACS Appl. Mater. Interfaces 10, 6652–6660. http://dx.doi.org/10.1021/acsami.7b13626.
Dores, R., Hussain, A., Katebah, M., Adham, S., 2012. Using advanced water treatment technologies to treat produced water from the petroleum industry. In: All Days. SPE, http://dx.doi.org/10.2118/157108-MS.
Hailan, S.M., Ponnamma, D., Krupa, I., 2021. The separation of oil/water mixtures by modified melamine and polyurethane foams: A review. Polym. 13, 4142. http://dx.doi.org/10.3390/POLYM13234142.
Han, L., Bi, H., Xie, X., Su, S., Mao, P., Sun, L., 2020. Superhydrophobic graphene-coated sponge with microcavities for high efficiency oil-in-water emulsion separation. Nanoscale 12, 17812–17820. http://dx.doi.org/10.1039/D0NR04892E.
Ho, Y.S., McKay, G., 1998. The kinetics of sorption of basic dyes from aqueous solution by sphagnum moss peat. Can. J. Chem. Eng. 76, 822–827. http://dx.doi.org/10.1002/CJCE.5450760419.
Hossain, M.A., Kumita, M., Michigami, Y., Mori, S., 1898. About the theory of so-called adsorption of soluble substances. Sven. Vetensk. Handingarl 24, 1–39. http://dx.doi.org/10.1252/JCEJ.38.402.
Hrubecky, H.F., 1958. Experiments in liquid atomization by air streams. J. Appl. Phys. 29, 572–578. http://dx.doi.org/10.1063/1.1723225.
Igunnu, E.T., Chen, G.Z., 2014. Produced water treatment technologies. Int. J. Low-Carbon Technol. 9, 157–177. http://dx.doi.org/10.1093/ijlct/cts049.
Jurado, E., Bravo, V., Camacho, F., Vicaria, J.M., Fernández-Arteaga, A., 2007. Estimation of the distribution of droplet size, interfacial area and volume in emulsions. Colloids Surf. A 295, 91–98. http://dx.doi.org/10.1016/J.COLSURFA.2006.08.037.
Khosravi, M., Azizian, S., 2016. A new kinetic model for absorption of oil spill by porous materials. Microporous Mesoporous Mater. 230, 25–29. http://dx.doi.org/10.1016/J.MICROMESO.2016.04.039.
Li, Jian, Li, D., Hu, W., Li, Jianping, Yang, Y., Wu, Y., 2015. Stable superhydrophobic and superoleophilic silica coated polyurethane sponges for the continuous capture and removal of oils from the water surface. New J. Chem. 39, 9958–9962. http://dx.doi.org/10.1039/C5NJ01565K.
Munirasu, S., Haija, M.A., Banat, F., 2016. Use of membrane technology for oil field and refinery produced water treatment—A review. Process Saf. Environ. Prot. 100, 183–202. http://dx.doi.org/10.1016/j.psep.2016.01.010.
Neff, J., Lee, K., DeBlois, E.M., 2011. Produced water: Overview of composition, fates, and effects. Prod. Water 3–54. http://dx.doi.org/10.1007/978-1-4614-0046-2_1.
Oliveira, L.M.T.M., Saleem, J., Bazargan, A., Duarte, J.L. da S., McKay, G., Meili, L., 2021. Sorption as a rapidly response for oil spill accidents: A material and mechanistic approach. J. Hazard. Mater. 407, 124842. http://dx.doi.org/10.1016/j.jhazmat.2020.124842.
Ong, C., Shi, Y., Chang, J., Alduraiei, F., Ahmed, Z., Wang, P., 2019. Polydopamine as a versatile adhesive layer for robust fabrication of smart surface with switchable wettability for effective oil/water separation. Ind. Eng. Chem. Res. 58, 4838–4843. http://dx.doi.org/10.1021/acs.iecr.8b06408.
Padaki, M., Surya Murali, R., Abdullah, M.S., Misdan, N., Moslehyani, A., Kassim, M.A., Hilal, N., Ismail, A.F., 2015. Membrane technology enhancement in oil–water separation. A review. Desalination 357, 197–207. http://dx.doi.org/10.1016/j.desal.2014.11.023.
Patterson, J.W., Patterson, J.W., 1985. Industrial Wastewater Treatment Technology, second ed. Butterworths, Boston.
Pinto, J., Athanassiou, A., Fragouli, D., 2018. Surface modification of polymeric foams for oil spills remediation. J. Environ. Manag. 206, 872–889. http://dx.doi.org/10.1016/j.jenvman.2017.11.060.
Pintor, A.M.A., Vilar, V.J.P., Botelho, C.M.S., Boaventura, R.A.R., 2016. Oil and grease removal from wastewaters: Sorption treatment as an alternative to state-of-the-art technologies. A critical review. Chem. Eng. J. 297, 229–255. http://dx.doi.org/10.1016/J.CEJ.2016.03.121.
Rahman, S.S., 1992. Evaluation of filtering efficiency of walnut granules as deep-bed filter media. J. Pet. Sci. Eng. 7, 239–246. http://dx.doi.org/10.1016/0920-4105(92)90021-R.
Ritger, P.L., Peppas, N.A., 1987a. A simple equation for description of solute release I. Fickian and non-fickian release from non-swellable devices in the form of slabs, spheres, cylinders or discs. J. Control. Release 5, 23–36. http://dx.doi.org/10.1016/0168-3659(87)90034-4.
Ritger, P.L., Peppas, N.A., 1987b. A simple equation for description of solute release II. Fickian and anomalous release from swellable devices. J. Control. Release 5, 37–42. http://dx.doi.org/10.1016/0168-3659(87)90035-6.
Saleem, J., Dotto, G.L., McKay, G., 2021. Current scenario and challenges in using plastic wastes as oil absorbents. J. Environ. Chem. Eng. 9, 104822. http://dx.doi.org/10.1016/j.jece.2020.104822.
Salvador, F., Martin-Sanchez, N., Sanchez-Hernandez, R., Sanchez-Montero, M.J., Izquierdo, C., 2015a. Regeneration of carbonaceous adsorbents. Part I: Thermal regeneration. Microporous Mesoporous Mater. 202, 259–276. http://dx.doi.org/10.1016/j.micromeso.2014.02.045.
Salvador, F., Martin-Sanchez, N., Sanchez-Hernandez, R., Sanchez-Montero, M.J., Izquierdo, C., 2015b. Regeneration of carbonaceous adsorbents. Part II: Chemical, microbiological and vacuum regeneration. Microporous Mesoporous Mater. 202, 277–296. http://dx.doi.org/10.1016/j.micromeso.2014.08.019.
Stejskal, J., Vilčáková, J., Jurča, M., Fei, H., Trchová, M., Kolská, Z., Prokeš, J., Křivka, I., 2022. Polypyrrole-coated melamine sponge as a precursor for conducting macroporous nitrogen-containing carbons. Coatings 12 (324), http://dx.doi.org/10.3390/coatings12030324.
Tanudjaja, H.J., Hejase, C.A., Tarabara, V.V., Fane, A.G., Chew, J.W., 2019. Membrane-based separation for oily wastewater: A practical perspective. Water Res. 156, 347–365. http://dx.doi.org/10.1016/j.watres.2019.03.021.
Wang, N., Wang, Y., Shang, B., Wen, P., Peng, B., Deng, Z., 2018. Bioinspired one-step construction of hierarchical superhydrophobic surfaces for oil/water separation. J. Colloid Interface Sci. 531, 300–310. http://dx.doi.org/10.1016/j.jcis.2018.07.056.
Weber, W.J., Morris, J.C., 1963. Kinetics of adsorption on carbon from solution. J. Sanit. Eng. Div. 89, 31–59. http://dx.doi.org/10.1061/JSEDAI.0000430.
Wenzel, R.N., 1936. Resistance of solid surfaces to wetting by water. Ind. Eng. Chem. 28, 988–994. http://dx.doi.org/10.1021/ie50320a024.
Yang, J., Wang, H., Tao, Z., Liu, X., Wang, Z., Yue, R., Cui, Z., 2019. 3D superhydrophobic sponge with a novel compression strategy for effective water-in-oil emulsion separation and its separation mechanism. Chem. Eng. J. 359, 149–158. http://dx.doi.org/10.1016/j.cej.2018.11.125.
Yin, Z., Li, Yuhang, Song, T., Bao, M., Li, Yiming, Lu, J., Li, Yang, 2020. An environmentally benign approach to prepare superhydrophobic magnetic melamine sponge for effective oil/water separation. Sep. Purif. Technol. 236, 116308. http://dx.doi.org/10.1016/j.seppur.2019.116308.
Zhang, L., Dong, D., Shao, L., Xia, Y., Zeng, T., Wang, Y., 2019. Cost-effective one-pot surface modified method to engineer a green superhydrophobic sponge for efficient oil/water mixtures as well as emulsions separation. Colloids Surf. A 576, 43–54. http://dx.doi.org/10.1016/j.colsurfa.2019.05.022.
Zhang, X.F., Song, L., Chen, X., Wang, Y., Feng, Y., Yao, J., 2020. Zirconium ion modified melamine sponge for oil and organic solvent cleanup. J. Colloid Interface Sci. 566, 242–247. http://dx.doi.org/10.1016/J.JCIS.2020.01.101.
Zhang, W., Wang, J., Han, X., Li, L., Liu, E., Lu, C., 2021. Carbon nanotubes and polydopamine modified poly(dimethylsiloxane) sponges for efficient oil–water separation. Materials (Basel) 14 (2431), http://dx.doi.org/10.3390/ma14092431.